Design of a Ducted Fan Aerial Robot for Simulating Weightless Objects

Mingjing Wang
School of Mechanical Engineering & Automation
Beihang University
Beijing, China
wangmj01@buaa.edu.cn

Long Li
School of Mechanical Engineering & Automation
Beihang University
Beijing, China
bhlilong@buaa.edu.cn

Xueying Jin
School of Mechanical Engineering & Automation
Beihang University
Beijing, China
xy_jin@buaa.edu.cn

Haoyuan Liu*
School of Mechanical Engineering & Automation
Beihang University
Beijing, China
liuhaoyuan2020@buaa.edu.cn

Chencai Wang
School of Mechanical Engineering & Automation
Beihang University
Beijing, China
cc_wang@buaa.edu.cn

Kun Xu
School of Mechanical Engineering & Automation
Beihang University
Beijing, China
xk007@buaa.edu.cn

Xilun Ding
School of Mechanical Engineering & Automation
Beihang University
Beijing, China
xlding@buaa.edu.cn

2024 9th International Conference on Automation, Control and Robotics Engineering (CACRE) | 979-8-3503-5030-2/24/$31.00 ©2024 IEEE | DOI: 10.1109/CACRE62362.2024.10635079

***Abstract*—Simulating the motion of objects under conditions of vacuum-induced weightlessness within terrestrial environments has long been a significant research direction in the field of aerospace, which holds substantial significance for operations involving space robotic arms, including cooperation, the capture of non-cooperative targets, and the defense against small celestial bodies. We propose a multi degree of freedom ducted fan quadcopter Aerial robot suitable for ground simulation of weightless objects. In response to the requirements for simulating the position and attitude of objects under weightlessness conditions, the structure of the aerial robot has been designed. The dynamic model of the aircraft has been established using the Newton Euler method, and the decoupling of attitude and position can be achieved through mechanism design and control algorithms. Compared with traditional quadcopter flying robots, the outer frame closed-loop control has been added, and the disturbance caused by the outer frame rotation on the fuselage has been addressed. Based on the original controller, a dynamic feedforward link was introduced, and the functionality of the prototype and the stability and speed of the control system were verified through experiments.**

Keywords—Aerial Robots, Weightlessness Simulation, Feedforward Anti-interference Control

I. INTRODUCTION

In the past decade, as a rapidly developing field, the research focus of aerial robots has gradually shifted from the flight control problem of drones to multi rotor drones with additional mechanical structures and multiple functions. [1] Industry level functional drones equipped with GPS, visual cameras, and other sensors are used in reconnaissance and surveillance, agricultural operations, aerial rescue, and other tasks.

It is a common work in the aerospace field to simulate the motion performance of objects in weightless environment in space. It can usually be used to test the function of aerospace products, such as micro satellites and free flying space robots (FFSR). In the past, pioneering methods for simulating weightless objects in the ground environment include Bremen tower and weightless aircraft in Germany based on free fall motion, mechanical arm simulation system based on hanging wire counterweight method proposed by Brown Hb to balance the gravity of objects [2], [3], Ranger test system developed by the University of Maryland uses water flotation to simulate zero gravity environment [4], while air flotation is often the most commonly used method to simulate the motion of weightless objects, such as ARL free flying robot test platform designed by Stanford University in the United States [5], and two-dimensional free flying satellite model robot proposed by Tokyo Institute of technology in Japan [6]. This method is easy to implement and has high simulation accuracy, but it has high cost for small and micro simulation test targets and lacks three-dimensional simulation. pace motion simulation.

At present, there are many models of laboratory prototype quadcopter drones and commercial products in the field of aerial robots. [7] In order to expand the aerial operation capability of drones and protect them, various structures, especially intelligent and freely controllable mechanisms, have been integrated into ordinary quadcopter platforms. Mellinger [8] studied the aerial grasping and operation of a quadcopter by attaching a gripping mechanism to the quadcopter of a hummingbird. Klaptocz [9] equipped rotary wing aircraft with an active upright mechanism and proposed a flying robot that can maintain upright performance at all times and prepare for takeoff after collision at the end of the mission. Kalantari and

Spenko[10] integrated a rolling cage into a quadcopter motherboard and proposed a hybrid ground and air quadcopter aircraft capable of both aerial and ground motion. Mintchev [11] developed a compact quadcopter with foldable and self-deployable arms using the concept of deployable structures. Liu [12] achieved the collection of eDNA from biological surfaces using aerial drones by attaching force sensing cages at the bottom of the drone. Ding [13] proposed a multi-propeller multifunction aerial robot (MMAR) capable of flying wall-climbing and arm-operating.

Therefore, based on the above research status, considering the urgent need for a lightweight ground simulation of the motion of weightless objects in space, and the advantages of using rotor lift to balance gravity, hovering, fast response speed, and high degree of freedom of motion of quadcopter flying robots, we conduct research on the ground simulation of weightless objects in space using quadcopter flying robots. Our work will provide a suitable simulation of weightless objects for grasping experiments of space robotic arms. The contributions of this article are as follows:1. A multi degree of freedom channel quadcopter aerial robot is designed for the ground simulation requirements of weightless objects in space environment.2. A dynamic model of the robot is established based on Newton Euler method, and outer frame closed-loop control and dynamic feedforward are introduced.3. The robot structure and control algorithm are verified through simulation and practical experiments. The following article is organized as follows: Chapter 2 discusses the structural design of the robot, Chapter 3 conducts kinematic and dynamic modeling of the robot, and Chapter 4 introduces the controller algorithm design of the robot and functional experiments conducted in simulation and practical environments.

II. Ductal Aerial Robot with Rotatable Frame

A. Design of the robot

We propose a quadcopter ducted drone with an integrated outer ring rotating frame. The aircraft integrates the two degrees of freedom rotational motion of the outer ring frame into the quadcopter through the transmission mechanism of the inner and outer rings. As shown in Figure 1, the micro servo 1 installed on the side of the drone is fixedly connected to the carbon fiber inner ring through carbon pipes and connectors, achieving the rotation of the inner ring around the Y-axis. The micro servo 2 is installed on the carbon fiber inner ring, the axis direction is at a 90 ° angle to servo 1 and is fixedly connected to the carbon fiber outer ring, thereby driving the rotation around the X-axis. The rotating frame is fixedly connected to the outer ring through 3D printed connectors arranged uniformly in a circumferential direction, ensuring two degrees of freedom rotation of the frame in a hovering state. In addition, passive rotating mechanisms are installed on the opposite sides of both servos to ensure a balanced configuration of the overall mass of the robot, keeping the center of gravity of the robot at the center of the frame and not changing with the rotation of the rotating frame. From the perspective of aerodynamic performance, the ducted fan motor has the advantages of a larger thrust to weight ratio and smaller size compared to ordinary rotor motors. It can improve the load redundancy of flight robots and is suitable for medium to high speed flight tasks. At the same time, it can provide protection for the motor and blades. Therefore, a ducted motor is used to enhance the power of the robot. [14]

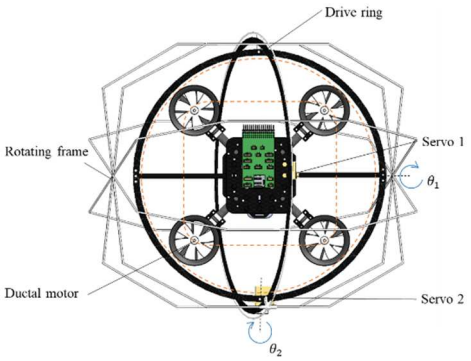

Fig. 1: Structure of the aerial robot

The main body structure and transmission inner and outer rings of the aircraft are made of carbon fiber material, and the rotating frame is made of 3D printed resin material. The main parameters of the drone are shown in TABLE I.

TABLE I: Structural parameters of the robot

parameters	mass	wheelbase	flight time	load
value	898 g	230 mm	4 min	3000 g

III. Kinematic and Dynamic Modeling

In order to better control the UAV in simulation and reality, and verify the motion performance and rotation function of the robot, the dynamic model of the quadrotor UAV with additional degrees of freedom is derived in this section, which has the following assumptions: the UAV structure and propeller are rigid, the center of gravity of the quadrotor aircraft coincides with the origin of the fuselage fixed frame, and does not change with the rotation of the frame (this is guaranteed in the structural design), according to the empirical formula of aerodynamics, the thrust of ducted motor is proportional to the square of propeller speed.

A. Kinematic Model

Firstly, the kinematics of the frame rotating quadrotor UAV is introduced to provide the basis for the dynamic model. Without losing generality, we select the plane parallel state of

the uniform fuselage on the upper layer of the inner and outer ring for analysis, and establish the global coordinate system (inertial coordinate system) $O_e - x_e y_e z_e$ and the fuselage coordinate system$O_b - x_b y_b z_b$, where the origin of the fuselage coordinate system coincides with the centroid of the structure, and its x_b axis points to the forward direction of the fuselage. As shown in Fig. 2.

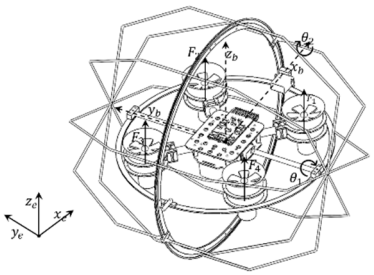

Fig.2: Four rotor coordinate system and cage coordinate system

The absolute position of the quadrotor UAV is defined as $p = \left[x\ y\ z\right]^T$, the attitude is defined by the rotation around the three axes of the fixed inertial coordinate system, and the roll angle ϕ around x_b Pitch angle θ around y_b, And the yaw angle ψ around z_b. Therefore, the relationship between the direction of the quadrotor and the inertial frame can be expressed by the rotation matrix.

$$R_b^e = \begin{bmatrix} c_\theta c_\psi & c_\psi s_\theta s_\phi - s_\psi c_\phi & c_\psi s_\theta c_\phi + s_\psi s_\phi \\ c_\theta s_\psi & s_\psi s_\theta s_\phi - c_\psi c_\phi & s_\psi s_\theta c_\phi - c_\psi s_\phi \\ -s_\theta & s_\phi c_\theta & c_\phi c_\theta \end{bmatrix} \quad (1)$$

Where s_x and c_x denote $sinx$ and $cosx$ respectively. And the RPY angle of UAV is defined as vector $\Theta = \left[\phi\ \theta\ \psi\right]^T$. Its Euler rate vector is $\omega_s = \left[\dot{\phi}\ \dot{\theta}\ \dot{\psi}\right]^T$. Angular velocity vector is $\omega_b = \left[p\ q\ r\right]^T$, the relationship between the two is:

$$\omega_b = \dot{R}(\phi)\begin{bmatrix}\dot{\phi}\\0\\0\end{bmatrix} + R(\phi)\dot{R}(\theta)\begin{bmatrix}0\\\dot{\theta}\\0\end{bmatrix} + R(\phi)R(\theta)\dot{R}(\psi)\begin{bmatrix}0\\0\\\dot{\psi}\end{bmatrix} \quad (2)$$

Consider the assumption of small angle change, that is, during flight $\left[\dot{\phi}\ \dot{\theta}\ \dot{\psi}\right]$ are very small, then $\dot{R}(\phi) = \dot{R}(\theta) = \dot{R}(\psi) = I$, where I is a 3 × 3 identity matrix. Therefore, from (2):

$$\begin{bmatrix}p\\q\\r\end{bmatrix} = \begin{bmatrix}1 & 0 & -s\theta\\0 & c\phi & s\phi c\theta\\0 & -s\phi & c\phi c\theta\end{bmatrix}\begin{bmatrix}\dot{\phi}\\\dot{\theta}\\\dot{\psi}\end{bmatrix} = T\omega_s \quad (3)$$

B. Dynamic Model

According to Newton Euler equation, the three-dimensional motion of a rigid body can be decomposed into translation and rotation around the center of mass. It is described by Newton's second law and Euler's equation respectively. First, the translation of the center of mass can be described according to Newton's second law, because the center of mass is only subject to the pull of gravity and propeller. Thus:

$$\boldsymbol{F} = m\frac{dv}{dt} = mg\boldsymbol{e_z} - f\mathbf{R_b^e}\boldsymbol{e_z} \quad (4)$$

Where $e_z = [0\ 0\ 1]^T$, f is the thrust generated by the propeller, g is the acceleration of gravity. The position dynamics model can be obtained by substituting the rotation matrix.

$$\begin{cases}\ddot{x} = -\frac{f}{m}(cos\psi sin\theta cos\phi + sin\psi sin\phi)\\ \ddot{y} = -\frac{f}{m}(sin\psi sin\theta cos\phi - cos\psi sin\phi)\\ \ddot{z} = g - \frac{f}{m}cos\phi cos\theta\end{cases} \quad (5)$$

The rotation of a rigid body around the center of mass is described according to Euler equation:

$$J\dot{\omega}_b + \omega_b \times (J\omega_b) = M_b \quad (6)$$

Where the mass product of the inertia term is *J,* and assuming that the aircraft structure is symmetrical, there is $J_{xy} = J_{xz} = J_{yz} = 0$, which can be substituted into the solvable attitude dynamics equation as

$$\begin{cases}\dot{p} = \frac{1}{J_x}\left[M_x + qr(J_y - J_z)\right]\\ \dot{q} = \frac{1}{J_y}\left[M_y + pr(J_z - J_x)\right]\\ \dot{r} = \frac{1}{J_z}\left[M_z + pq(J_x - J_y)\right]\end{cases} \quad (7)$$

Considering that the aircraft is flying at a low speed, the airflow resistance and tilting moment can be ignored. According to the aerodynamic principle of quadrotor aircraft and the previous assumptions:

$$\begin{cases}f = K_T(\Omega_1^2 + \Omega_2^2 + \Omega_3^2 + \Omega_4^2)\\ M_x = \frac{\sqrt{2}}{2}K_T l(-\Omega_1^2 + \Omega_2^2 + \Omega_3^2 - \Omega_4^2)\\ M_y = \frac{\sqrt{2}}{2}K_T l(\Omega_1^2 + \Omega_2^2 - \Omega_3^2 - \Omega_4^2)\\ M_z = K_Q(\Omega_1^2 - \Omega_2^2 + \Omega_3^2 - \Omega_4^2)\end{cases} \quad (8)$$

Where Ω_i represents the speed of motor i, K_T is the total coefficient of rotor lift, and K_Q is the total coefficient of rotor torque. l is the distance between the center of mass and the motor shaft.

On the basis of the dynamic model of the four rotors flight platform, it is necessary to consider the impact on the dynamic

performance after installing the rotating frame. The rotating frame is connected with the flight platform through the inner and outer transmission rings and the steering gear. Since the steering gear is fixed on the axis of the aircraft when it is installed, it can be assumed that during the rotation process, the first rudder will generate a Y-axis reverse torque M_{servoY} to the aircraft, and the second rudder will generate an X-axis reverse torque M_{servoX} to the aircraft. Therefore, the position dynamics of the whole aircraft remains unchanged, and the attitude dynamics equation is rewritten as:

$$\begin{cases} \dot{p} = \frac{1}{J_x}\left[M_x + qr(J_y - J_z) + M_{servoX}\right] \\ \dot{q} = \frac{1}{J_y}\left[M_y + pr(J_z - J_x) + M_{servoY}\right] \\ \dot{r} = \frac{1}{J_z}\left[M_z + pq(J_x - J_y)\right] \end{cases} \tag{9}$$

C. Dynamics Simulation

We use MATLAB script to simulate the dynamic model of the above four rotor aircraft and the aircraft loaded with rotating frame, observe the changes of aircraft attitude and position under different motor speeds, and analyze the specific impact of the rotation of the simulated shell and transmission mechanism on the attitude of the aircraft. The physical parameters and coefficients are shown in TABLE II.

TABLE II: SIMULATION PARAMETERS

parameters	value	parameters	value
J_x	$3.65 \times 10^{-3} kg \cdot m^2$	K_T	5.7×10^{-7}
J_y	$5.08 \times 10^{-3} kg \cdot m^2$	K_Q	6×10^{-8}
J_z	$6.61 \times 10^{-3} kg \cdot m^2$	l	115 mm

Firstly, the dynamic response at different throttle is analyzed, in which the throttle input and motor speed approximately meet the linear relationship under the condition of high throttle, but the motor speed has response time to the throttle input, which can be approximated as a first-order system and has the following formula:

$$\frac{T_m d\Omega(t)}{dt} + \Omega(t) = C_m \delta(t) + \Omega_m \tag{10}$$

Where T_m is the time required for the motor speed to reach 63.2% of the stable speed, taking the common value of 127ms. C_m is the motor speed at full throttle, Ω_m is the motor speed at zero throttle, that is, the motor speed intercept. The simulation results are shown in Fig.3 (a), which respectively represent the throttle centering($\delta_i = 0.5$) and full throttle($\delta_i = 1$).The lifting force F, roll moment M_x, pitch moment M_y and yaw moment M_z can be seen from the simulation results that the lifting force of the aircraft under the condition of full throttle is about 30N, that is, the load is 3000g, which is consistent with the design results, and the lifting force is about 9N under the condition of half throttle, which is just balanced with the actual mass of the UAV to achieve hovering. In the ideal case, when the four motors have the same speed, only lift will be generated without torque to change the attitude and X Y position, which is also consistent with the actual four rotor physical flight principle.

Next, consider the impact on the dynamic performance of the aircraft after installing the rotating frame, and substitute the value into the simulation program, as shown in Fig. 3(b)

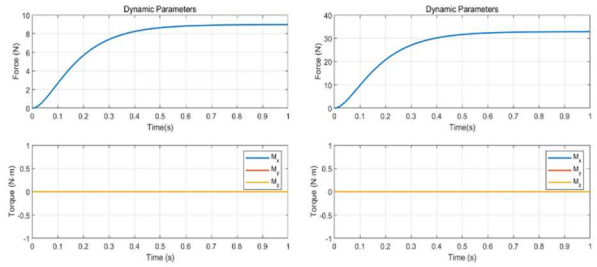

(a) Dynamic response of throttle centering and full throttle

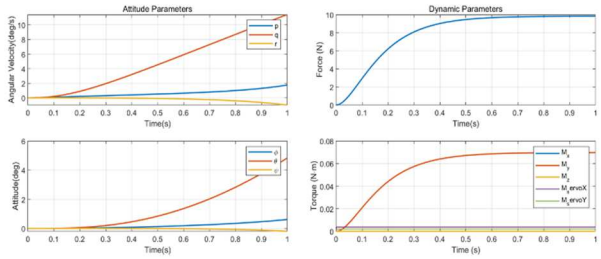

(b) Dynamic attitude response curve with rotating frame

Fig.3: Dynamics simulation

IV. CONTROL SYSTEM AND FUNCTIONAL VERIFICATION

According to the dynamic model established above, the position PD control of the inner and outer loop and the attitude PID controller with feedforward are designed for the flight control of the UAV. The inner loop is attitude control and the outer loop is position control. The control scheme is shown in Fig.4.

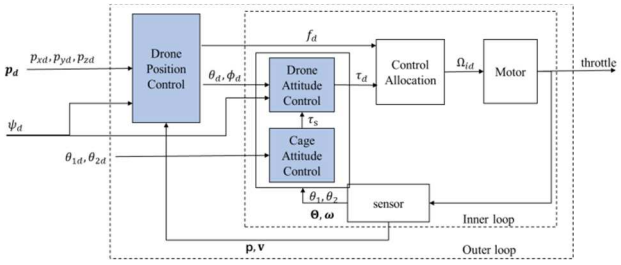

Fig.4: Control system (p_d, ψ_d, θ_d, ϕ_d f_d represents the desired position, desired yaw angle, desired pitch angle, desired roll angle, and desired lift respectively, τ_s is feedforward torque)

A. Position Control

According to the control system in the figure above, first of all, it is necessary to design a position controller according to

the known expected position $p_d$and yaw angle ψ_d. The desired pitch angle and roll angle for attitude control are obtained ϕ_d, θ_d and the desired pulling force f_d for motor control distribution. Because the application scenario of the aircraft in our work is mainly in the low-speed stable flight state, the input of the position dynamics model can be simplified as follows:

$$f = mg, \tau = 0 \tag{11}$$

Generally, the pitch angle and roll angle are not too large, so the following small angles can be used:

$$sin\phi \approx \phi, cos\phi \approx 1, sin\theta \approx \theta, cos\theta \approx 1, \psi \approx \psi_d \tag{12}$$

Where $A_\psi = \begin{bmatrix} cos\psi & -sin\psi \\ sin\psi & cos\psi \end{bmatrix}\begin{bmatrix} 0 & 1 \\ -1 & 0 \end{bmatrix}, \boldsymbol{\Theta_h} = \begin{bmatrix} \phi \\ \theta \end{bmatrix}, \boldsymbol{p_h} = \begin{bmatrix} p_x \\ p_y \end{bmatrix}$,The position dynamics after approximate treatment is as follows:

$$\begin{cases} \ddot{p}_h = -gA_\psi \Theta_h \\ \ddot{p}_z = g - \dfrac{f}{m} (\neq 0) \end{cases} \tag{13}$$

Then the PD control of the horizontal channel $p_h = [p_x, p_y]^{\mathrm{T}}$ can be designed as follows:

$$\boldsymbol{\Theta_{hd}} = -\mathrm{g}^{-1} A_\psi^{-1} \left(\ddot{p}_{hd} + K_D (\dot{p}_{\mathrm{hd}} - \dot{p}_h) + K_P (p_{hd} - p_h) \right) \tag{14}$$

This gives the desired pitch and roll angles $\boldsymbol{\Theta_{hd}} = [\phi_d \ \theta_d]^T$.

The PD controller of the altitude channel can also be designed as follows:

$$f_d = mg - m\left(\ddot{p}_{zd} + K_D (\dot{p}_{\mathrm{zd}} - \dot{p}_z) + K_P (p_{zd} - p_z) \right) \tag{15}$$

The desired lift f_d is given by the above (14) (15) which is the position PD controller established based on the aircraft position dynamics model.

B. Attitude Control

The purpose of aircraft attitude control is to design a controller to obtain the desired torque according to the known desired pitch, roll and yaw angles. The desired pitch and roll angles are given by the position controller, and the desired yaw angle is given by the mission planning. For the attitude dynamics model given in (9), considering that the attitude angular velocity is also small when the aircraft is flying at low speed and small angle, the cross terms pr, qr, pq of the angular velocity can be ignored, so the attitude dynamics model of the aircraft is obtained as follows:

$$\begin{cases} \dot{p} = \dfrac{1}{J_x} [M_x + M_{servoX}] \\ \dot{q} = \dfrac{1}{J_y} [M_y + M_{servoY}] \\ \dot{r} = \dfrac{1}{J_z} M_z \end{cases} \tag{16}$$

The matrix form is:

$$\boldsymbol{J\dot{\omega}} = \boldsymbol{\tau} + \begin{bmatrix} M_{servox} \\ M_{servoy} \\ \mathbf{0} \end{bmatrix} \tag{17}$$

Since the attitude angle value is the Euler angle obtained by gyroscope and IMU attitude calculation and EKF filtering, there is error and delay [15]. In order to speed up the response speed of attitude control, the angular velocity value compensation angle measured by the sensor can be used as the control inner loop in the attitude control process. At the same time, setting the angular velocity control loop can also make the three items of PID control have physical significance and higher control accuracy. Firstly, the attitude angle P control is designed to obtain the desired attitude angular velocity:

$$\boldsymbol{\omega_d} = K_P (\boldsymbol{\Theta_d} - \boldsymbol{\Theta}) \tag{18}$$

Then the feedforward attitude angular velocity PID control based on balanced actuator torque can be designed, where $\boldsymbol{e_\omega} = \boldsymbol{\omega_d} - \boldsymbol{\omega}$,

$$\boldsymbol{\tau_d} = K_P \boldsymbol{e_\omega} + K_I \int \boldsymbol{e_\omega} + K_D \dot{\boldsymbol{e}}_{\boldsymbol{\omega}} + \begin{bmatrix} M_{servox} \\ M_{servoy} \\ \mathbf{0} \end{bmatrix} \tag{19}$$

Feedforward quantity $\tau_s = \begin{bmatrix} M_{servox} \\ M_{servoy} \\ \mathbf{0} \end{bmatrix}$ obtained by PID control of servo angle:

$$\tau_{\mathrm{s}} = K_P \boldsymbol{e_i} + K_I \int \boldsymbol{e_\omega} + K_d \dot{\boldsymbol{e}}_{\boldsymbol{i}} \tag{20}$$

Where $\boldsymbol{e_i} = \boldsymbol{\theta_{id}} - \boldsymbol{\theta_i}$, θ_{1d} Indicates the target position (angle) of the outer ring actuator rotation.

Equation (18) (19) (20) above is the feedforward PID attitude controller based on the overall aircraft attitude dynamics model.

C. Functional Verification

Firstly, the functional flight simulation of the aircraft model is carried out in the gazebo simulation software, and the robot operating system (ROS) is used to establish the control system according to the previous control model to control the position and attitude of the aircraft. During flight, the quadrotor platform moves in three degrees of freedom and yaw spin, and the rotating frame rotates in two degrees of freedom during flight, as shown in Fig.5 and Fig.6.

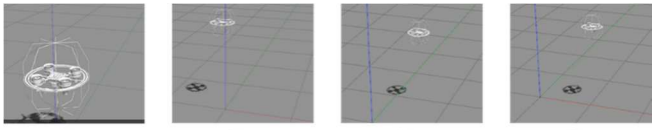

Fig.5: Three degree of freedom translation in Gazebo

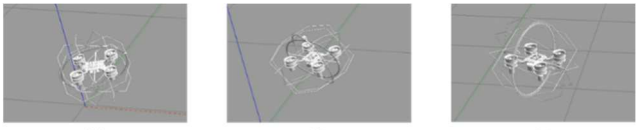

Fig.6: Two degrees of freedom rotation of the cage in Gazebo

From the simulation results, the accuracy of the flight principle of the prototype is verified, and the fixed-point movement of the aircraft in the XYZ axis direction is realized.

During the flight process, the yaw spin and two degrees of freedom rotation through the transmission ring are realized through the four rotors, and finally the six degrees of freedom movement of the rotating frame in space is realized. The expected function of simulating the six degree of freedom motion of space weightlessness object is verified.

On the basis of simulation, the actual verification prototype is established. On the basis of passing the early flight performance test and rotation function test, the six degree of freedom motion function of the outer ring frame is realized on the real prototype, and the performance and maneuverability of the robot are verified. As shown in Fig.7.

Fig.7: Robot functional test (a) three degree of freedom movement and spin rotation test of quadrotor flight platform (b) two degree of freedom rotation test of rotating frame on the ground (c) six degree of freedom movement test of the whole robot

From the data recorded in the robot flight test (Fig.8), it can be observed that the control and tracking effect of roll angle and pitch angle is good, with an average error of 0.19 ° in roll angle control and an average adjustment time of 0.12 seconds; The average error of pitch angle control is 0.33 °, and the average adjustment time is 0.28 seconds. This verifies the stability and robustness performance of the control system. The attitude controller based on feedforward has a good control effect on the disturbance of roll and pitch angle caused by the rotation of the cage during flights, and will not cause interference to the flight of the quadcopter platform.

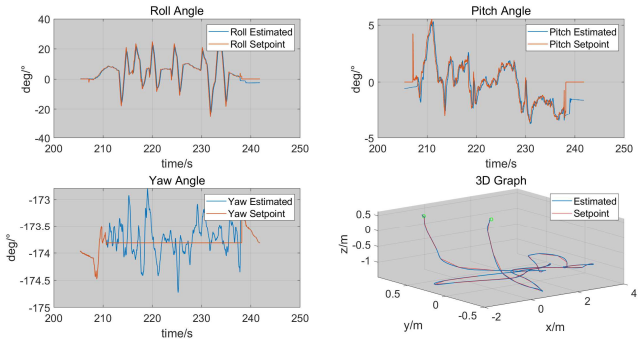

Fig.8: Attitude and position tracking data

V. Conclusion

In our work, we propose a quadcopter with a fully free motion frame for ground simulation of weightless object motion. To achieve multi configuration switching and six degree of freedom motion of the outer ring frame during the flight process, in order to more realistically simulate the multi degree of freedom motion of space weightless objects. The structural design of the quadcopter aircraft was introduced, and a robot dynamics model was established based on the Newton Euler method for the robot. On this basis, outer frame control and dynamic feedforward links were introduced to improve the aerial trajectory tracking effect of the robot under controlled outer frame rotation conditions. Finally, the motion performance and tracking stability of the control system of the robot were verified through robot prototype in realistic experiments. The tracking errors of roll and pitch angles are both within 0.5°. The adjustment time of about 0.3 seconds verified the quick-response of the control system.

Acknowledgment

This research was funded by the National Natural Science Foundation of China (NSFC No. U22B2080). Thanks to the experiment participants for their help and Space Robot Laboratory of BUAA for its support to this study.

[1] Meng, Jiawei, et al. "On aerial robots with grasping and perching capabilities: A comprehensive review." Frontiers in Robotics and AI 8 (2022): 739173.

[2] Brown H B, Dolan J M. A novel gravity compensation system for space robots[C]. ASCE, 1994.

[3] Xu Y, Brown H B, Friedman M, et al. Control system of the self-mobile space manipulator[J]. IEEE Transactions on Control Systems Technology, 1994, 2(3): 207-219.

[4] Parrish J C Ranger telerobotic shuttle experiment (RTSX): status report[J]. Proceedings of SPIE - The International Society for Optical Engineering.

[5] Russakow J, Rock S M, Khatib O. An operational space formulation for a free-flying, multi-arm space robot[J]. Lecture Notes in Control & Information Sciences, 1997, 223:448-457.

[6] Umetani Y, Yoshida K. Experimental study on two-dimensional free-fly ing robot satellite model. 1989.

[7] S. N. Ghazbi, Y. Aghli, M. Alimohammadi and A. A. Akbari, "Quadrotors unmanned aerial vehicles: a review", International Journal on smart sensing and intelligent system, vol. 9, pp. 309-333, 2016.

[8] D. Mellinger, Q. Lindsey, M. Shomin and V. Kumar, "Design modelling estimation and control for aerial grasping and manipulation", 2011 IEEE/RSJ International Conference on Intelligent Robots and Systems,

[9] Wang, J. "Fundamentals of erbium-doped fiber amplifiers arrays (Periodical style—Submitted for publication)." IEEE J. Quantum Electron (2005).

[10] A. Klaptocz, L. Daler, A. Briod, J.-C. Zufferey and D. Floreano, "An active uprighting mechanisms for flying robots", IEEE Transactions on Robotics, vol. 28, pp. 1152-1157, 2012.

[11] S. Mintchev, L. Daler, G. L'Eplattenier, L. Saint-Raymond and D. Floreano, "Foldable and self-deployable pocket-sized quadrotor", 2015 IEEE International Conference on Robotics and Automation (ICRA),

[12] Haoran Liu,Hongmiao Tian,Duorui Wang,Tengfei Yuan,Jinyu Zhang,Guifang Liu,Xiangming Li,Xiaoliang Chen,Chunhui Wang,Shengqiang Cai,Jinyou Shao,Electrically active smart adhesive for a perching-and-takeoff robot, Science Advances, 9, 43, (2023).

[13] Ding X, Yu Y, Zhu J J. Trajectory linearization tracking control for dynamics of a multi-propeller and multifunction aerial robot-MMAR[C]//2011 IEEE International Conference on Robotics and Automation. IEEE, 2011: 757-762.

[14] Fan, Wei, et al. "Adaptive fault-tolerant control of a novel ducted-fan aerial robot against partial actuator failure." Aerospace science and technology 122 (2022): 107371.

[15] Quan, Quan, and Kai-Yuan Cai. "Additive-output-decomposition-based dynamic inversion tracking control for a class of uncertain linear time-invariant systems." 2012 IEEE 51st IEEE Conference on Decision and Control (CDC). IEEE, 2012.